Catalysis Letters Vol. 110, Nos. 1–2, August 2006 (© 2006)
DOI: 10.1007/s10562-006-0086-y

Studies on cobalt catalyst supported on silica with different pore size for Fischer–Tropsch synthesis

Hualan Li, Jinlin Li,* Hekai Ni, and Dechen Song

Key Laboratory of Catalysis and Materials Science of Hubei Province, College of Chemistry and Materials Science, South-Central University for Nationallities, Wuhan 430074, China

Received 12 December 2005; accepted 3 May 2006

Mesoporous molecular sieves (MCM-48, SBA-15 and SiO_2) with different pore diameters have been used as supports of Co catalysts for Fischer–Tropsch (F–T) synthesis. The catalysts were characterized by N_2 physisorption, X-ray diffraction (XRD), temperature programmed reduction (TPR), temperature programmed desorption (H_2 TPD) followed by pulse oxygen reoxidation and transmission electron microscopy (TEM). The catalytic performace for FT synthesis was tested with a fixed bed reactor. TEM and H_2 TPD showed that the cobalt crystallite size formed on Co/SBA-15 with the pore diameter of 5.3 nm were the largest, and the ones formed on Co/MCM-48 with pore diameter of 2.6 nm were the smallest. The Co/SiO_2 with the average pore diameter at 10.4 nm is most active for FTS. The Co/SBA-15 presented the highest selectivity to C5+. The activity of the three catalysts was affected by the reducibility of cobalt oxides and C5+ selectivity was determined by the cobalt crystallite size.

KEY WORDS: Fischer–Tropsch synthesis; MCM-48; SBA-15; SiO_2; cobalt; catalyst.

1. Introduction

The Fischer–Tropsch synthesis (FTS) can convert coal-based and/or natural gas-derived syngas into ultra-clean, sulfur-free chemicals and fuels. Supported cobalt catalysts have been found to be promising catalysts for FTS. In order to gain high metal dispersion, cobalt is typically supported on oxides with high surface area, such as silica, alumina, titania and zeolites. Non-uniformities in the support pore size distributions may lead to differences in the hydrocarbon products distribution. Recently, well-defined mesoporous molecular sieves have been used as the support to prepare cobalt based catalysts. There include MCM-41 [1–3], SBA-15 [3–5], and HMS [6]. The effect of porosity of support on the chain growth probability factor and reactant/product diffusion rates was important in F–T synthesis.

Iwasaki *et al.* [7] used SCMM1 and SCMM2 while Khodakov *et al.* [1] used MCM-41, SBA-15 and commercial mesoporous silicas supports for Co catalysts. They found the FTS reaction rate and C5+ selectivity increased with increasing catalyst pore size. Khodakov and co-workers [1,8,9] found Co/SBA-15 catalysts to be more active and selective toward C5+ hydrocarbons than Co/MCM-41, and ascribed this to a higher reducibility of the larger Co_3O_4 particles formed in the larger pores of SBA-15 support. Saib *et al.* [10] also reported that the catalyst supported by silica with average pore diameter of 10 nm was the most active and has high selectivity for hydrocarbon formation. The C5+ selectivity was a maximum, while methane selectivity was minimum at a pore diameter of 10 nm. Ernst *et al.* [11] found the activity of Co/SiO_2 catalysts for FTS increased with the specific surface area, and the selectivity for long chain hydrocarbons was favored in the case of the catalyst with support pore diameter less than 4.0 nm.

The above studies indicated that the pore size of catalyst affects product selectivity, through the spatial effects of the support. Catalyst supports with small pores can achieve higher dispersion of supported cobalt crystallites due to higher support surface area. Catalyst supports with wide pores can diminish the diffusion resistance and provide pathways for rapid molecular transport [12]. However, the effect of physical and chemical properties of supports on the performances of Co catalysts in FT synthesis still remains unclear [1]. In this work, we have undertaken a thorough study of cobalt-supported mesoporous MCM-48, SBA-15, SiO_2 catalysts with different pore diameters ranging from 2.6 to 10.4 nm. The catalytic behaviors of these catalysts for the FTS were determined. The catalysts were characterized by N_2 physisorption, X-ray diffraction (XRD), transmission electron microscopy (TEM), temperature programmed reduction (TPR), hydrogen temperature programmed desorption (H_2-TPD) and O_2 pulse reoxidation. The influence of pore size on the distribution of cobalt species and catalytic properties of Co/MCM-48, Co/SBA-15 and Co/SiO_2 catalysts were investigated.

*To whom correspondence should be addressed.
E-mail: lij@scuec.edu.cn

2. Experimental

MCM-48 was synthesized by the conventional hydrothermal pathway similar to the procedure described previously [13]. *n*-Hexadecyltrimethylammonium bromide ($C_{16}H_{33}(CH_3)_3$-NBr) was dissolved in deionized water, and sodium hydroxide and tetraethoxysilane (TEOS) were added. The molar composition of TEOS: NaOH:$C_{16}H_{33}(CH_3)_3$-NBr:H_2O was 1:0.48:0.4:55. The solution was stirred for about 30 min, charged into a polypropylene bottle and then heated at 383 K for 3 days. The sample was filtered, washed with water, and calcined at 773 K for 6 h to remove template.

SBA-15 was synthesized through a process that has been described in detail elsewhere [14]. An acidic aqueous mixture of a triblock copolymer (Aldrich), poly(ethylene oxide)–poly(propylene oxide)–poly(ethylene oxide) (EO_{20}–PO_{70}–EO_{20}), trimethylbenzene, and tetraethyl orthosilicate was first heated at 308 K for 24 h, followed by post synthesis treatment at 370 K for 24 h. Then, the synthesized SBA-15 was separated by filtration, followed by repeated washing with distilled water, subsequently dried at room temperature, and lastly calcined in air at 773 K for 6 h.

SiO_2 support used was commercial silica (Meigao Co.Ltd. China). The calcined MCM-48, SBA-15 and SiO_2 (impurities were not detectable in the analysis) were used as supports for the Co catalyst.

Co was introduced to the supports by incipient wetness impregnation using aqueous solutions of cobalt nitrate. After impregnation the catalysts were dried at 373 K for 12 h and then calcined in a flow of air. The MCM-48 and SBA-15 supported catalysts were calcined at 773 K for 5 h. The SiO_2 supported catalyst was calcined at 723 K for 5 h. All three catalysts were prepared with 15 wt% cobalt loading and denoted as Co/MCM-48, Co/ SBA-15, and Co/SiO_2, respectively.

2.1. Characterization techniques

BET measurements: Pore size distribution, BET surface area and total pore volume (TPV) were measured by nitrogen physisorption using a Micromeritics ASAP 2405 automatic system at 77 K. The specific surface area was estimated by the BET method. The pore size distribution and pore volume was determined by the BJH method [15].

XRD: X-ray diffraction patterns were obtained at room temperature using a Phillips X'pert diffractometer with monochromatic Cu–Kα radiation. The scan range was 1$\sim$80° with 0.002° steps. The average particle sizes of Co_3O_4 were estimated from the Scherrer equation [16] using the most intense reflection at $2\theta = 36.9°$

2.1.1. Temperature programmed reduction (TPR)

The catalyst reduction behavior and the interaction between active phase and supports were examined by TPR in a Zeton Altamira AMI-200 unit. Prior to the hydrogen TPR measurement, the catalyst was flushed with high purity argon at 423 K for 1 h, and cooled down to 323 K. Then 10% H_2/Ar was passed through the catalyst at a total flow rate of 30 cm^3 min^{-1} while the temperature was increased to 1023 K at a rate of 10 K min^{-1}. A computer recorded automatically the H_2 consumption (TCD signal).

2.1.2. Hydrogen temperature programmed desorption (H_2-TPD) and pulse O_2 reoxidation

Hydrogen temperature programmed desorption was also performed using the Zeton Altamira AMI-200 unit. The catalyst was reduced at 723 K for 12 h using high purity hydrogen and then cooled to 373 K under hydrogen flow. The sample was held at 373 K for 1 h under flowing argon to remove weakly bound physisorbed species. Then, the temperature was slowly increased to 723 K at a ramp rate of 10 K min^{-1}, the catalyst was held under flowing argon to desorb the remaining chemisorbed hydrogen and the TCD began to record the signal until the signal returned to the baseline.

O_2 pulse reoxidation was also performed with the Zeton Altamira AMI-200 unit. After reduction under the conditions as described above for the H_2-TPD, the catalyst was kept in flowing Ar at 723 K and the sample was reoxidized by injecting pulses of high purity oxygen in argon. The reducibility was calculated by assuming that metal Co was oxidized to Co_3O_4.

Using hydrogen TPD to assess the number of surface cobalt atoms available, and the pulse reoxidation experiment to determine the extent of cobalt reduction, the corrected cobalt cluster size (and therefore, corrected dispersion) was estimated. The formula for the calculation has been described previously [17–19] and the results are shown in table 3.

2.1.3. Transmission electron microscopy (TEM)

Transmission electron microscopy characterization of the catalyst was carried out using a FEI Tecnai $G^2$20 instrument. The catalyst was crushed in an agate mortar, dispersed in ethanol and dropped on copper grids. The Co_3O_4 average crystallite size and crystallite-size distributions were obtained by TEM. Between 100 and 300 particles coming from at least three images were measured, the statistical average was calculated from these data. Thus, only a rough indication on the cobalt particle size can be given, due to the limited number of TEM images.

2.1.4. Fischer–Tropsch synthesis reaction

The performance of catalysts in the FTS was tested in a fixed bed reactor at 503 K and 10 bar. Catalyst (6 g) mixed with 36.0 g carborundum were loaded into the reactor. Catalyst was reduced in H_2 *in situ* at atmospheric pressure at 723 K for 12 h. Subsequently, the reactor was cooled down to 453 K. The flow of hydrogen and carbon monoxide (H_2:CO = 2:1) was introduced

and the pressure was increased to 10 bar. The reactor temperature was increased to 503 K in 4 h and the reaction was carried out at 503 K. The effluent product gas was passed through an Agilent 3000 GC for online analysis. The products were collected in a hot trap and a cold trap in sequence. The carbon monoxide conversion (X_{CO}%) was measured at steady state. X_{CO}% and hydrocarbon selectivity were averaged over the period of constant operation.

3. Results and discussion

3.1. Catalyst and support porosity

The pore size distribution profiles for the three catalysts are shown in figure 1. BET surface areas, TPV, and average pore diameters of all the supports and catalysts listed in table 1. The shapes of N_2 desorption isotherms for the catalysts were similar to that of the original MCM-48, SBA-15 and SiO_2. It suggested that the mesoporous structure of supports were mostly retained upon cobalt impregnation. Figure 1 indicates a wider pore size distribution in SiO_2 than MCM-48 and SBA-15. Figure 1 also shows the mean pore diameter ranged from 2.6 nm in the MCM-48 to 10.4 nm in the SiO_2 support. Table 1 shows both the BET surface areas, pore volumes and mean pore diameter of the catalysts decreased after loading Co, especially Co/MCM-48.

3.2. Cobalt species and crystallite sizes

X-ray diffraction patterns were collected at both lower and higher diffraction angles. Diffraction peaks at 2θ of 31.3°, 36.9°, 45.1°, 59.4° and 65.4° indicate that after calcination, cobalt was present in the form of crystalline Co_3O_4 spinel on all the catalysts and Co species are highly dispersed. The MCM-48 and Co/MCM-48 provided two distinct diffraction lines due to SiO_2 (211), (220) planes, showing cubic structures [20].

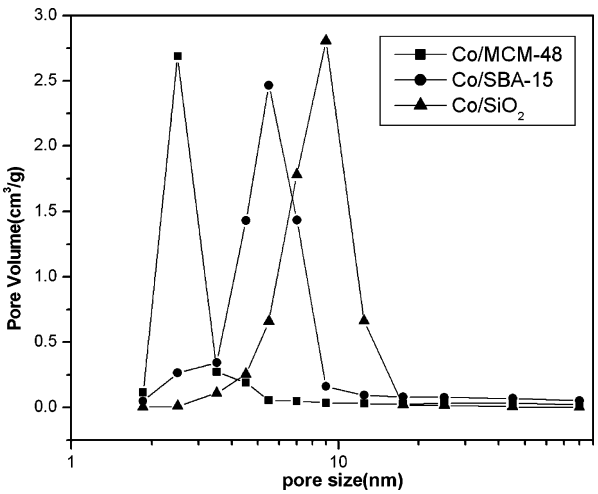

Figure 1. Pore size distribution of catalysts.

SBA-15 and Co/SBA-15 showed three well-resolved diffraction peaks which can be indexed as the (100), (110) and (200) reflections associated with *p6mm* hexagonal symmetry [14]. After loading Co, the reflection intensity decreased greatly, but the catalysts still retained the regular mesoporous structure.

Significant differences in crystallite-size distributions obtained by TEM for three catalysts are shown in figure 2. When the pore size of the support increased, the maximum in the crystallite size distribution shifted toward larger size. The distributions for Co/SBA-15 showed a bimodal pattern. For comparison, the crystallite size obtained by XRD, TPD and TEM methods are shown in table 2. Usually the Co_3O_4 particles size increased with increasing pore size of the support. The average Co_3O_4 particle sizes detected were larger than the corresponding pore diameters, indicating that Co_3O_4 clusters are formed outside the pores. From the data obtained from TEM or TPD, the Co_3O_4 crystallites is smallest for Co/MCM-48 and largest for Co/SBA-15. The cobalt crystallite diameter calculated from XRD for the three catalysts was larger than detected from the other methods. It was probably because of the following reasons. First, it is known that some very small cobalt particles could be missed by XRD. Second, the Scherrer equation used to calculate crystallite sizes from the width of XRD patterns, could overestimate the sizes of crystallite particles [21]. Some cobalt crystallites exited as very small particles inside the small pore of MCM-48 where H_2 chemisorption might have been partially blocked and missed by XRD. So Co_3O_4 crystallite size of Co/MCM-48 from XRD and TPD methods might be overestimated significantly.

3.3. Cobalt reducibility

The TPR profiles for the catalysts are shown in figure 3. Table 3 lists the extent of Co reduction and Co^0 dispersion estimated from TPD and O_2 reoxidation. From figure 3 the three catalysts have similar reduction profiles with two main reduction peaks, which are close to each other temperature less than 723 K. The first peak could be assigned to the reduction of Co_3O_4 to CoO, and the second peak corresponds to the subsequent reduction of CoO to Co^0 [22]. Co/SBA-15 and Co/MCM-48 catalysts show the third small reduction feature at 733–823 K that can be considered as the reduction of the smaller cobalt oxide particles observed by TEM. Co/MCM-48 catalyst showed a fourth reduction peak with a temperature above 900 K, which may reflect the reduction of cobalt silicates [23].

Khodakov *et al.* [24] suggested that the interaction between cobalt and support in smaller particles was much stronger than in larger particles and this interaction was likely to stabilize small oxidized particles and clusters in silica. From the crystallite diameter data obtained by TEM, the sequence of increasing small

Table 1
N_2 physisorption results

Silica	S_{BET}[a] (m^2/g)	TPV[b] (cm^3/g)	Pore diameter (nm)	Co catalysts	S_{BET}[a] (m^2/g)	TPV[b] (cm^3/g)	Pore diameter (nm)
MCM-48	1127	1.1	2.6	Co/MCM-48	626	0.58	2.4
SBA-15	662	0.88	5.3	Co/SBA-15	453	0.595	5.2
SiO_2	350	0.87	10.4	Co/SiO2	285	0.7	10.1

[a]BET surface area; [b]Total pore volume.

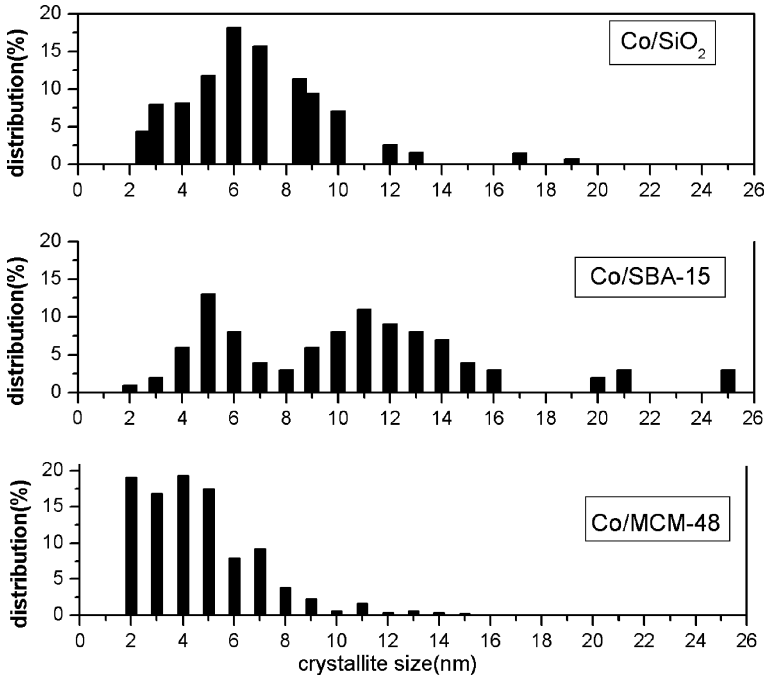

Figure 2. Cobalt crystallite size distributions as determined by TEM.

crystallite diameter below 5 nm is Co/SiO_2 < Co/SBA-15 < Co/MCM-48. This particle distribution might explain the different H_2 reducing behavior that was displayed by the different number of H_2 reduction peaks shown in figure 3. Interactions between smaller cobalt particles and SiOH groups in the SBA-15 and MCM-48 supports may retard reduction to Co^0. It is known that larger cobalt crystallite can be easily reduced to cobalt metal which is active for FTS. So the reducibility sequence is Co/SiO_2 > Co/SBA-15 > Co/MCM-48, which is in agreement with the amount of chemisorbed H_2 by TPD method and results of O_2 pulse reoxidation.

Table 2
Average cobalt crystallite size on the catalysts

Catalyst	Average cobalt crystallite diameter (nm)			Most frequently crystallite size[a] (nm)
	XRD	TPD[a]	TEM	TEM
Co/MCM-48	14	9.6	6.8	2∼ 5
Co/SBA-15	14.8	11.7	8	4∼ 6, 9∼ 14
Co/SiO_2	14.3	6.7	7	6∼ 10

[a]Data from figure 2.

3.4. Fischer–Tropsch synthesis reaction

3.4.1. Activity of the catalysts

CO conversion and the selectivity to the different FTS products are presented in table 4. CO conversion increased with increasing average pore size. Co/MCM-48 catalyst presented the lowest CO conversion. Small particles could be easily reoxidized by water and other reaction products and thus become inactive under FT synthesis [25]. Poor reducibility of small Co crystallites confined within the mesoporous channels of MCM-48 support may explain the relatively low activity of Co/MCM-48. The Co/SiO_2 with the largest average pore diameter of 10.4 nm has the highest CO conversion and highest reducibility which could lead to a greater density of active surface Co^0 sites, as can be seen from the H_2 desorbed data listed in table 3. An increase in the mean crystallite size and reducibility of cobalt particles with increasing average pore size has also been observed for a series of Co/SiO_2 catalysts with varied pore diameter [10].

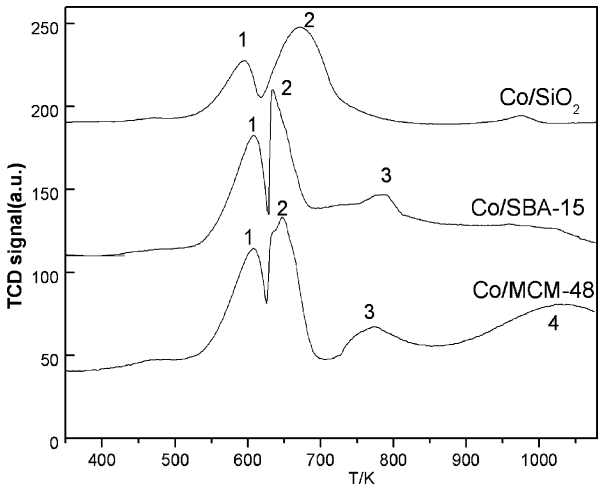

Figure 3. TPR Profiles of catalysts.

3.4.2. Product selectivity

In general, the C5+ selectivity increases with increasing CO conversion. But from table 4, the Co/SBA-15 gives the highest selectivity to C5+ and Co/MCM-48 catalyst displays the highest methane and lowest C5+ selectivity. As shown in table 3, most of cobalt crystallite size is 2∼ 5 nm for Co/MCM-48. Khodakov *et al.* [1] found an inverse relationship between the methane selectivity and the extent of overall reduction for cobalt-supported mesoporous silicas. The higher methanation activity of Co/MCM-48 may lead to its low C5+ selectivity. Girardon *et al.* [26] reported that the unreduced oxide phase could catalyze water–gas shift reaction increasing the effective H_2/CO ratio which would result in high yield of carbon dioxide and methane. Lapszewicz *et al.* [27] reported that the diffusion limitations for carbon monoxide in catalysts pore could increase H_2/CO ratio in catalyst pore and thus increase the methane selectivity.

Saib *et al.* [10] reported that the catalyst supported by commercial silica with average pore diameter of 10 nm was the most active and selective catalyst in FTS. They found the C5+ and methane selectivity passed through a maximum and minimum, respectively, at the 10 nm pore size. However, our results are not in agreement with the results reported by Saib *et al.* [10]. We found that Co/SBA-15 with the pore size at 5.3 nm displayed the highest C5+ selectivity. It is generally considered [28,29] that the presence of larger cobalt particles leads to higher selectivity to heavier hydrocarbons. Iglesia [25] also suggested diffusion-enhanced readsorption of the primary α-olefins which could join in the chain-growing processes favoring the formation of longer hydrocarbon chains. But Zhan and Davis considered [30] that there is not only diffusivity of the products but also the higher solubility in the liquid phase of heavy hydrocarbons which tended to accumulate in the catalyst pores. Barbier *et al.* [31] studied the influence of cobalt particle size from 4 to 10 nm for FTS and found that the chain growth probability first increases rapidly and then more slowly for cobalt particle diameter larger than 6 nm, and their data showed that Co/SiO_2 catalyst with cobalt particle diameter at 9 nm displayed high chain growth probability and low rate of deactivation. The highest selectivity of Co/SBA-15 seemed to correlate the presence of a higher proportion of larger cobalt particles, as shown in table 2 and figure 2. In this study, the three catalysts seemed to agree with the cobalt crystallite size sensitivity for FTS. But it is known that catalytic properties of cobalt catalysts supported on silica are affected by the porosity and structure of support. It is possible that the regular mesorporous pore structure of SBA-15 has a beneficial effect on mass transfer. In fact, we cannot deduce the true conclusion only using the above data. We are doing the H_2/D_2 switch test for FTS, and hope to obtain the correct product distribution and verify these phenomena in the future.

Table 3
H_2-TPD and pulse O_2 reoxidation data

Catalyst	H_2 desorbed (μmol/g)	O_2 uptake (μmol/g)	Co^0 dispersion (%)	Extent of reduction (%)
Co/MCM-48	40.4	471	14.2	21.3
Co/SBA-15	42	476.4	11.7	28
Co/SiO2	94	655.7	23.4	51

Table 4
Catalytic results for FTS on the catalysts

Catalyst	$X_{(CO)}$,%[a]		Hydrocarbon selectivity (mol%)					
	Initial	Steady	$S(CO_2)$[b]	C_1	C_2	C_3	C_4	C_{5+}
Co/MCM-48	27.2	25.8	1.44	17.79	1.13	2.79	2.07	74.78
Co/SBA-15	61.8	59.4	1.32	10.97	0.56	1.13	0.84	85.18
Co/SiO_2	64.9	63.2	1.7	14.1	1.25	1.18	0.8	80.97

[a]CO conversion.
[b]CO_2 selectivity.
The catalysts were reduced in a flow of H_2 at 723 K for 12 h before FTS.
Reaction conditions: $H_2/CO = 2$, $T = 230$ °C, $P = 10$ bar., space velocity of syngas: 2 S L g^{-1} h^{-1} (273 K, 0.1 Mpa).

4. Conclusions

Catalytic behavior of cobalt catalyst supported on silica in FT synthesis depended on cobalt species, cobalt particle size and support mesoporous structure. The Co_3O_4 crystallites sizes were controlled by the support pore diameters in mesoporous silicas. The order of decreasing average Co_3O_4 crystallite diameter was Co/SBA-15 > Co/SiO_2 > Co/MCM-48, and the C5+ selectivity for the three catalysts followed this sequence. The low reducibility of the large amount of small cobalt particles and cobalt silicates formed on Co/MCM-48 led to the lowest activity and C5+ selectivity. The low dispersion for Co/SBA-15 led to the loss of active cobalt metal sites. Meanwhile the Co/SiO_2 had moderate cobalt particle size and the highest dispersion. The sequence of deceasing CO hydrogenation activity was Co/SiO_2 > Co/SBA-15 > Co/MCM-48.

Acknowledgments

The work was supported by the National Natural Science Foundation of China (20473114, 20590360), Talented Young Scientist Foundation of Hubei (2003ABB013), Excellent Young Teachers Program of Ministry of Education of China, the State Ethnic Affairs Commission, P.R. China and Returnee Startup Scientific Research Foundation of Ministry of Education of China.

References

[1] A.Y. Khodakov, A. Griboval-Constant, R. Bechara and V.L. Zholobenko, J. Catal. 206 (2002) 230.
[2] J. Panpranot, J.G. Goodwin Jr. and A. Sayari, Catal. Today 77 (2002) 269.
[3] Y. Ohtsuka, Y. Takahashi, M. Noguchi, T. Arai, S. Takasaki, N. Tsubouchi and Y. Wang, Catal. Today 89 (2004) 419.
[4] Y. Wang, M. Noguchi, Y. Takahashi and Y. Ohtsuka, Catal. Today 68 (2001) 4.
[5] A.Y. Khodakov, R. Bechara and A. Griboval-Constant, Appl. Catal. A Gen. 254 (2003) 273.
[6] D. Yin, W. Li, H. Xiang, Y. Sun, B. Zhong and S. Peng, Micropor. Mesopor. Mater. 47 (2001) 15.
[7] T. Iwasaki, M. Reinikainan, Y. Onodera, H. Hayashi, T. Ebina, T. Nagase, K. Torii, K. Kataja and A. Chatterjee, Appl. Surf. Sci. 130–132 (1998) 845.
[8] A. Griboval-Constant, A.Y. Khodakov, R. Bechara and V.L. Zholobenko, Stud. Surf. Sci. Catal. 144 (2002) 609.
[9] A.Y. Khodakov, R. Bechara and A. Griboval-Constant, Stud. Surf. Sci. Catal. 142 (2002) 1133.
[10] A.M. Saib, M. Claeys and E. van Steen, Catal. Today 71 (2002) 395.
[11] B. Ernst, S. Libs, P. Chaumette and A. Kiennemann, Appl. Catal. A Gen. 186 (1999) 145.
[12] M. Shinoda, Y. Zhang, Y. Yoneyama, K. Hasegawa and N. Tsubaki, Fuel Process Technol. 86 (2004) 73.
[13] S.G. Wang, D. Wu, Y.H. Sun and B. Zhong, Mater. Res. Bull. 36 (2001) 1717.
[14] D.Y. Zhao, J.L. Feng, Q.S. Huo, N. Melosh, G.H. Fredrickson, B.F. Chmelka and G.D. Stucky, Science 279 (1998) 548.
[15] E.P. Barrett, L.G. Joyner and P.P. Halenda, J. Am. Chem. Soc. 73 (1951) 373.
[16] B.D. Cullity, *Elements of X-Ray Diffraction* (Addision-Wesley, London, 1978).
[17] H.F. Xiong, Y.H. Zhang, J.L. Li and Y.Y. Gu, J. Cent. South Univ. T. 11(4) (2004) 414.
[18] G. Jacobs, T.K. Das, Y.Q. Zhang, J.L. Li, G. Racoillet and B.H. Davis, Appl. Catal. A 233 (2002) 263.
[19] D. Schanke, S. Vada, E.A. Blekkan, A.M. Hilmen, A. Hoff and A. Holmen, J. Catal. 156 (1995) 85.
[20] C.T. Kresge, M.E. Leonowicz, W.J. Roth, J.C. Vartuli and J.S. Beck, Nature 359 (1992) 710.
[21] P. Ganesan, H.K. Kuo, A. Saaverda and R.J. DeAngelis, J. Catal. 52 (1978) 319.
[22] H. Ming and B.G. Baker, Appl. Catal. A 123 (1995) 23.
[23] B. Sexton, A. Hughes and T. Turney, J. Catal. 97 (1986) 390.
[24] A.Y. Khodakov, J. Lynch, D. Bazin, B. Rebours, N. Zanier, B. Moisson and P. Chaumette, J. Catal. 168 (1997) 16.
[25] E. Iglesia, Appl. Catal. A 161 (1997) 59.
[26] J.S. Girardon, A.S. Lermontov, L. Gengembre, P.A. Chernavskii, A.G. Constant and A.Y. Khodakov, J. Catal. 230 (2005) 339.
[27] M. Kraum and M. Baerns, Appl. Catal. A Gen. 186 (1999) 189.
[28] R.C. Reuel and C.H. Bartholomew, J. Catal. 85 (1984) 78.
[29] H.H. Nijs and P.A. Jacobs, J. Catal. 65 (1980) 328.
[30] X. Zhan and B.H. Davis, Appl. Catal. A Gen. 236 (2002) 149.
[31] A. Barbier, A. Tuel, I. Arcon, A. Kodre and G.A. Martin, J. Catal. 200 (2001) 106.